






Understanding Dynamics of Pandemic Models to Support Predictions of COVID-19 Transmission: Parameter Sensitivity Analysis of SIR-Type Models

Chunfeng Ma , Member, IEEE, Xin Li , Senior Member, IEEE, Zebin Zhao , Feng Liu , Kun Zhang, Adan Wu , and Xiaowei Nie

Abstract—Despite efforts made to model and predict COVID-19 transmission, large predictive uncertainty remains. Failure to understand the dynamics of the nonlinear pandemic prediction model is an important reason. To this end, local and multiple global sensitivity analysis approaches are synthetically applied to analyze the sensitivities of parameters and initial state variables and community size (N) in susceptible-infected-recovered (SIR) and its variant susceptible-exposed-infected-recovered (SEIR) models and basic reproduction number (R_0), aiming to provide prior information for parameter estimation and suggestions for COVID-19 prevention and control measures. We found that N influences both the maximum number of actively infected cases and the date on which the maximum number of actively infected cases is reached. The high effect of N on maximum actively infected cases and peak date suggests the necessity of isolating the infected cases in a small community. The protection rate and average quarantined time are most sensitive to the infected populations, with a summation of their first-order sensitivity indices greater than 0.585, and their interactions are also substantial, being 0.389 and 0.334, respectively. The high sensitivities and interaction between the protection rate and average quarantined time suggest that protection and isolation

measures should always be implemented in conjunction and started as early as possible. These findings provide insights into the predictability of the pandemic models by estimating influential parameters and suggest how to effectively prevent and control epidemic transmission.

Index Terms—Sensitivity analysis, pandemic, COVID-19, susceptible-exposed-infected-recovered (SEIR).

I. INTRODUCTION

CORONAVIRUS disease 2019 (COVID-19) has undoubtedly unprecedentedly threatened the health of people worldwide [1]–[3] and global economic development [4]–[6]. Although the pandemic has lasted for more than two years, scientific and public health communities are still making great effort on tracing its origination and predicting the future trends of the disease to protect human health and recover the global economy. Thus, timely monitoring and accurately predicting the evolution of the pandemic has been and will be a “new normal” task for the scientific and public health communities. Modeling and predicting COVID-19 transmission by using various mathematical models have attracted substantial attention from the scientific community [7]–[11], since the mathematical model plays an important role to better understand the disease dynamics, hence to making prevention and control policy to alleviate the spreading of disease [12]–[14].

Among many mathematical modelling methods, the most representative epidemic susceptible-infectious-recovered (SIR) model [15] and its various variants, e.g., the susceptible-exposed-infectious-recovered (SEIR) model [8], [9], [16], have been constantly improved and widely applied in predicting the spreading trends of the COVID-19 disease. The models have been witnessed a success in predicting the short-term spread of the pandemic, but large uncertainties remain in the long-term prediction [9]. Thus, quantifying these uncertainties could be informative to improve the predictability of the models as well as to provide suggestion for the policymaker to propose prevention and control measures.

It is found that the SIR-type model performance depends heavily on the initial values of the state variables and the parameters [7], [9], [17], especially on influential parameters

Manuscript received October 22, 2021; revised February 22, 2022; accepted April 16, 2022. Date of publication April 22, 2022; date of current version June 6, 2022. This work was supported in part by the Alliance of International Science Organizations under Grants ANSO-SBA-2020-13 and ANSO-SBA-2021-05, in part by the National Natural Science Foundation of China under Grant 41701418, and in part by the CAS Light of West China Program. (Corresponding author: Xin Li.)

Chunfeng Ma, Zebin Zhao, Feng Liu, and Adan Wu are with the Key Laboratory of Remote Sensing of Gansu Province, Northwest Institute of Eco-Environment and Resources, Chinese Academy of Sciences, Lanzhou 730000, China (e-mail: machf@lzb.ac.cn; zhaozebin@lzb.ac.cn; liufeng@lzb.ac.cn; wuadan@lzb.ac.cn).

Xin Li is with the National Tibetan Plateau Data Center, State Key Laboratory of Tibetan Plateau Earth System, Environment and Resources, Institute of Tibetan Plateau Research, Chinese Academy of Sciences, Beijing 100101, China (e-mail: xinli@itpcas.ac.cn).

Kun Zhang is with the Department of Mathematics, The University of Hong Kong, Pokfulam, Hong Kong, SAR 999077, China (e-mail: kunzh@hku.hk).

Xiaowei Nie is with the State Key Laboratory of Tibetan Plateau Earth System, Resources and Environment, Institute of Tibetan Plateau Research, Chinese Academy of Sciences, The Alliance of International Science Organizations, Beijing 100101, China (e-mail: xwnie@anso.org.cn).

Digital Object Identifier 10.1109/JBHI.2022.3168825

such as infectious rate. Under this context, a sensitivity analysis is required to quantify the relative contribution of model state variables and the parameters to the model outputs. Through the sensitivity analysis, not only can the modeler optimize the model by accurately estimating the influential parameters and initial values of the state variables, but also can we provide the policymaker with useful information to control the influential parameter.

Although many efforts have been made to quantify the impact of model parameters on model prediction, most of these efforts used local sensitivity analysis, e.g., Phaijoo and Gurung [18], Naveed *et al.* [19] and Resmawan and Yahya [20]. The local method that changes one factor at one time cannot identify the interactions among parameters. Besides, the sensitivity of a parameter may change when other parameters values change. Since SIR-type models are highly nonlinear models that do not have analytic solutions, global sensitivity analysis is needed to quantify the sensitivity of a single parameter and the interaction with others. This merit of the global sensitivity analysis is undoubtedly useful to clarify the co-effect among different parameters. Marino *et al.* [21] performed a global sensitivity analysis to biological system models to assess the uncertainty in the models. As to SIR-type models, several published work reported the use of global sensitivity analysis. For example, the Latin Hypercube Sampling scheme [22], [23] was applied to sample input and calculate the basic reproduction number (R_0), and partial rank correlation coefficients [24] were calculated to analyze the parameter sensitivity to basic reproduction number, but these work did not calculate the parameter sensitivity indices. Borgonovo and Lu [25] used three sensitivity measures to identify the parameter importance, but the interaction among parameters was not analyzed. Additionally, analyzing the effects of initial values of the state variable and community size on actively infected cases could inform new comprehension of the spread of the pandemic, but there are few analyses focusing on this issue. Thus, in addition to model parameters, we here simultaneously analyze the sensitivities of initial values of the state variables to model outputs.

Besides, the basic reproduction number [26], [27], defined as the average number of secondary infected cases generated by a primary case, is an important factor that determines the transmissibility [28]. If the basic reproduction number smaller than 1, infection-free steady state is globally asymptotically stable and the pandemic would not outbreak, otherwise, the pandemic inevitably outbreaks [29]. Thus, accurately estimating the basic reproduction number and identifying its influential parameters are equally important [30], [31]. To this end, we also conducted a global sensitivity analysis of parameters to the basic reproduction number, aiming to comprehensively understand its impact on the COVID-19 pandemic.

To comprehensively understand the model behavior and influence of parameters on model output and basic reproduction number, we investigate the effects of both state variables and the parameters in the SIR and SEIR models and those govern the basic reproduction number by performing both local and global sensitivity analyses. This paper aims to provide insights into how to improve the predictability of the model [32], [33] and to

TABLE I
DEFINITION OF STATE VARIABLES AND PARAMETERS

		Meaning
States	N	Total number of people
	S	Number of susceptible people
	E	Number of exposed people
	I	Number of infected people not quarantined
	R	Number of recovered people
	Q	Number of infected people in quarantine
	D	Number of the dead people
Parameters	P	Number of protected people
	α	Protection rate
	β	Infectious rate
	γ^{-1}	Average incubation
	δ^{-1}	Average quarantined time
	λ	Cure rate
	κ	Mortality rate

provide implications on how to effectively prevent and control epidemic transmission.

II. MATERIALS AND METHODS

A. SIR and SEIR Models

Two models, SIR and modified SEIR (hereinafter referred to as SEIR), are applied to sensitivity analysis. The former is the classic model, without introducing intervention measures; the latter introduces intervention measures. The influence of intervention measures on the model dynamics is expected to be identified by comparing the sensitivity analysis results of the two models. A SIR model is an epidemiological model that computes the number of infected people with a contagious illness in a closed population over time. The model involves coupled equations relating the number of susceptible (S), infected (I) and removed (R) people [34]. The SIR model is formulated as follows:

$$\frac{dS(t)}{dt} = -\beta \frac{S(t)I(t)}{N} \quad (1)$$

$$\frac{dI(t)}{dt} = \beta \frac{S(t)I(t)}{N} - \lambda I(t) \quad (2)$$

$$\frac{dR(t)}{dt} = \lambda I(t) \quad (3)$$

where the meanings of the model state variables and parameters are listed in Table I.

Different from the classic SIR model, the SEIR model introduces several states of population, such as exposed (E), quarantined (Q), and protected (P) populations [9], [35]. It also introduces intervention measures and parameters, such as the protection rate (α), by which suggestions for protecting the potentially susceptible population to support the control and prevention of the pandemic can be provided. The SEIR model is formulated as follows (also see Table I for the details of the

model state variables and parameters).

$$\frac{dS(t)}{dt} = -\beta \frac{S(t)I(t)}{N} - \alpha S(t) \quad (4)$$

$$\frac{dE(t)}{dt} = \beta \frac{S(t)I(t)}{N} - \gamma E(t) \quad (5)$$

$$\frac{dI(t)}{dt} = \gamma E(t) - \delta I(t) \quad (6)$$

$$\frac{dQ(t)}{dt} = \delta I(t) - \lambda Q(t) - \kappa Q(t) \quad (7)$$

$$\frac{dR(t)}{dt} = \lambda Q(t) \quad (8)$$

$$\frac{dD(t)}{dt} = \kappa Q(t) \quad (9)$$

$$\frac{dP(t)}{dt} = \alpha S(t) \quad (10)$$

Based on the modified SEIR model, the basic reproduction number (R_0) is formulated by [27]:

$$R_0 = \left(1 + \frac{\ln(Y(t)/t)}{\gamma}\right) \left(1 + \frac{\ln(Y(t)/t)}{\lambda}\right) \quad (11)$$

where $Y(t)$ is the number of infected populations by time t . Thus, the parameters that govern the behavior of the basic reproduction number are the same as those of infected populations.

B. Sensitivity Analysis Methods

Both local and global sensitivity analysis methods are applied in this research. Local sensitivity analysis is the simplest and most used method that qualitatively assesses the sensitivity of a single parameter on the model output by changing one factor at a time. Local sensitivity analysis is straight forward so that it sensibly visualizes the variation in model outputs depending on the specific parameter, but it cannot simultaneously quantify the sensitivity of multiple parameters, especially the interaction among parameters. As an alternative, the global sensitivity analysis method can quantitatively evaluate the sensitivity of all selected inputs and their interactions on the model outputs. To ensure the sensitivity analysis conducted here reliable and reasonable, two sensitivity analysis methods are exploited. Including the so-called Sobol's method [36], [37] and an extended Fourier amplitude sensitivity test (FAST) method [38]–[40], which are suitable for quantifying the first-order effect, the total effects and the interaction of parameters.

1) Local Sensitivity Analysis: Local sensitivity analysis evaluates the influence of a single input parameter on the model outputs at one time. A local sensitivity index is mathematically the partial derivative of model outputs concerning an individual parameter. In our present specific analysis, we analyze the sensitivity of parameters and initial values of the state variables in the SIR and SEIR models by observing the changes in the infected and cumulative cases through changing one of the inputs at one time.

2) Sobol's Method: Sobol's method is a global sensitivity analysis method that is based on the variance decomposition

technique. The method can simultaneously quantify the first-order effect (main sensitivity index, MSI) and total effect (total sensitivity index, TSI) of all input parameters at one time [36], [37]. The MSI, TSI and the interaction are calculated by:

$$MSI_i = \frac{V_i}{V} \quad (12)$$

$$TSI_i = 1 - \frac{V_{-i}}{V} \quad (13)$$

$$\sum_{i=1, j \neq i}^n S_{i,j} = TSI_i - MSI_i \quad (14)$$

where V_i , V_{-i} and V are respectively the first-order variance, variance without considering the i^{th} parameter and total variance in the model outputs. The relation between V_i and V is described as:

$$V = \sum_{i=1}^n V_i + \sum_{1 < i < j < n} V_{i,j} + \dots + \sum V_{1,2,\dots,n} \quad (15)$$

The second term on the right side of the equation represents the summation of high-order (including second order) variances. Without considering the 3rd-order to higher-order interactions, the second-order sensitivity index (S2) can be computed by subtracting the MSI from the TSI. In this paper, the MSI, TSI, and S2 are computed based on Sobol's method for the analysis.

3) FAST Method: The new version FAST applied here was proposed by Saltelli *et al.* [38] who combined the merit of the version of original FAST proposed in 1973 [41] and Sobol' method [36], [37]. The calculations of MSI and TSI in FAST method are with the same formulation as the Sobol' method. The advantage of FAST over the Sobol' method is that it applies a more efficient sampling strategy along a curve in the sample space, thus significantly improving the computing efficiency. More details regarding the performance and specification of the FAST method can be referred to references of Saltelli *et al.* [38].

C. Experimental Design

1) Sensitivity Analysis Using Local Method: In view that the calculation of R_0 is relatively simple, we do not conduct local sensitivity analysis on it. Thus, the local sensitivity analysis is conducted on SIR and SIER models. In the SIR model, in addition to the parameters (β , λ), we also analyze the influences of initial values of the state variables (I_0 , N) on the development of the infected populations. We observe the date on which the maximum number of actively infected cases reached and the maximum number of actively infected cases. Two experiments are attempted.

Experiment 1: Sensitivities of parameters and state variables on actively infected cases within a city-level community. This experiment characterizes the response of actively infected cases to the parameters and initial values of state variables changing at a moderate size of community, e.g., within a city level with a population of 1–2 million, where the initially infected cases number from hundreds to thousands. The experiment changes the values of I_0 , N , β , and λ to the same order of magnitude to determine how the number of actively infected cases changes.

Specifically, to analyze the initially infected populations on the variation in actively infected cases number, we change I_0 from 200 to 1000 ($I_0 = 1$ is also included) with a step of 200 while fixing N , β , and λ to 10,00000, 0.6, and 0.04, respectively, according to Nguemdjo *et al.* [42], where the parameters were estimated using a maximum likelihood estimation and data collected from a population of 25 million. Similarly, to see the community size on the variation in actively infected cases number, we change N from 1000000 to 2000000 with a step of 250000 while setting I_0 , β , and λ to 20, 0.6 and 0.04, respectively. We also change β from 0.2 to 1.0 with a step of 0.2 while fixing N , I_0 , and λ to 1000000, 200 and 0.04 and change λ from 0.02 to 0.1 with a step of 0.02 while fixing N , I_0 , and β to 1000000, 200, and 0.6, respectively. Through these changes in parameters β and λ , we analyze the influences of these parameters on the infected populations.

Experiment 2. Sensitivities of parameters and state variables on actively infected cases in communities of varying sizes. This experiment focuses on the changes in actively infected cases when the pandemic spreads in communities of different sizes, aiming to test the impact of community size on the actively infected cases and the pandemic time, i.e., to observe how the actively infected cases change when the pandemic spreads from a small (e.g., a village or a street level) to a large community (e.g., a country level). In this experiment, the values of the parameters and state variables are changed at interorders of magnitude, e.g., I_0 , ranging from 20 to 2000 with a step of $\times 10i$ ($i = 1, 2, 3 \dots$), N ranging from 10000 to 1000000, β ranging from 0.006 to 0.6 and λ ranging from 0.003 to 0.3.

Experiment 3. Local sensitivity analysis to identify how the parameter sensitivity changes when intervention measures are applied using the SEIR model. In the SEIR model, the intervention measures are applied by introducing the parameters of protection rate (α), average incubation time (γ^{-1}) and average quarantined time (δ^{-1}) in this experiment. We analyze the influences of these parameters together with the infection rate (β) on the actively infected and cumulatively infected cases. The parameters of cure rate (λ) and mortality rate (κ) are not directly related to the actively infected population in the SEIR model, so we exclude them from this analysis. The variation ranges of the parameter are determined by referring to Zhao *et al.* [9] with a minor change. Four attempts are conducted in this analysis: 1) α changing from 0.085 to 0.185 with a step of 0.02, with others taken as constant ($\beta = 0.78$, $\gamma = 0.2$, $\delta = 0.12$, $\lambda = 0.3$, $\kappa = 0.025$), 2) β changing from 0.5 to 1.0 with a step of 0.1, with $\alpha = 0.125$ and others the same as above (hereinafter), 3) γ changing from 0.1 to 0.35 with a step of 0.05, and 4) δ changing from 0.08 to 0.18 with a step of 0.02.

2) Sensitivity Analysis Using Global Method: Global sensitivity analyses (both Sobol's and FAST method) are conducted on the SEIR model and R_0 to quantify the sensitivities of all parameters at one time and their interactions. Additionally, the state variables are not included in this analysis because their influences have been analyzed in the local method and found to be insensitive to the infected population. Community size (N) is not included here either in global sensitivity analysis because its larger ranges (millions to billions) compared to the parameters

TABLE II
INITIAL VALUES (RANGES) IN THE MODIFIED SEIR MODEL FOR GLOBAL SENSITIVITY ANALYSIS

		Initial values/ranges	Reference
States	N	14,000,000	Statistics of Wuhan
	S	13,999,293	N-E-I-Q-D-P
	E	318	Statistics of Wuhan
	I	389	Statistics of Wuhan
	R	0	Statistics of Wuhan and [9]
	Q	700	Statistics of Wuhan
	D	0	Statistics of Wuhan and [9]
	P	0	Statistics of Wuhan and [9]
Parameters	α	0.085–0.183	[9] and [35]
	β	0.7–1.0	[9] and [35]
	γ^{-1}	5~7	[9] and [35]
	δ^{-1}	7~14	[9] and [35]
	λ	0.1~0.5	[9] and [35]
	κ	0.001~0.05	[9] and [35]

The initial values of the state variables and ranges of parameters are set according to the findings in [9] and [35]

(0–1) may influence the reasonability of the sensitivity analysis. In the global sensitivity analysis, two experiments (Experiments 4 & 5) are designed using Sobol's and FAST global sensitivity analysis methods.

Experiment 4: Global sensitivity analysis to quantify the parameter sensitivities and to rank parameter importance. This experiment is designed to calculate the parameter sensitivity indices (SIs) at a specific stage of the pandemic to provide an order of parameter importance. In this experiment, the initial values of the state variables and ranges of parameters are set in Table II according to the findings in [9] and [35]. To ensure the reliability of the analysis, parameters are uniformly distributed within the given ranges. The first-order effect (MSI), total effect (TSI) and interaction of parameters are quantified simultaneously. Parameter importance is ranked according to the obtained SIs, which are utilized to inform model parameter estimation and the prevention and control measures of the pandemic.

Experiment 5: Variation in parameter SIs to inform adjustments to prevention and control measures. This experiment is designed to observe the changes in the parameter SIs at different stages of the pandemic, which benefits adjusting the prevention and control measures at different stages of the pandemic. To investigate the temporal variation in parameter SIs, the state variables from the 5th day to the 180th day with a step of 5 days are exploited, and the ranges of parameters are set as those in Experiment 4.

III. RESULTS AND DISCUSSION

A. Parameter Sensitivity Based on Local Method

Experiment 1: When the parameters and state variables vary at the same order of magnitude, they lead to different maximum actively infected cases (I_{max}) and the day on which the maximum -cases reaches (D_{max}) (Fig. 1).

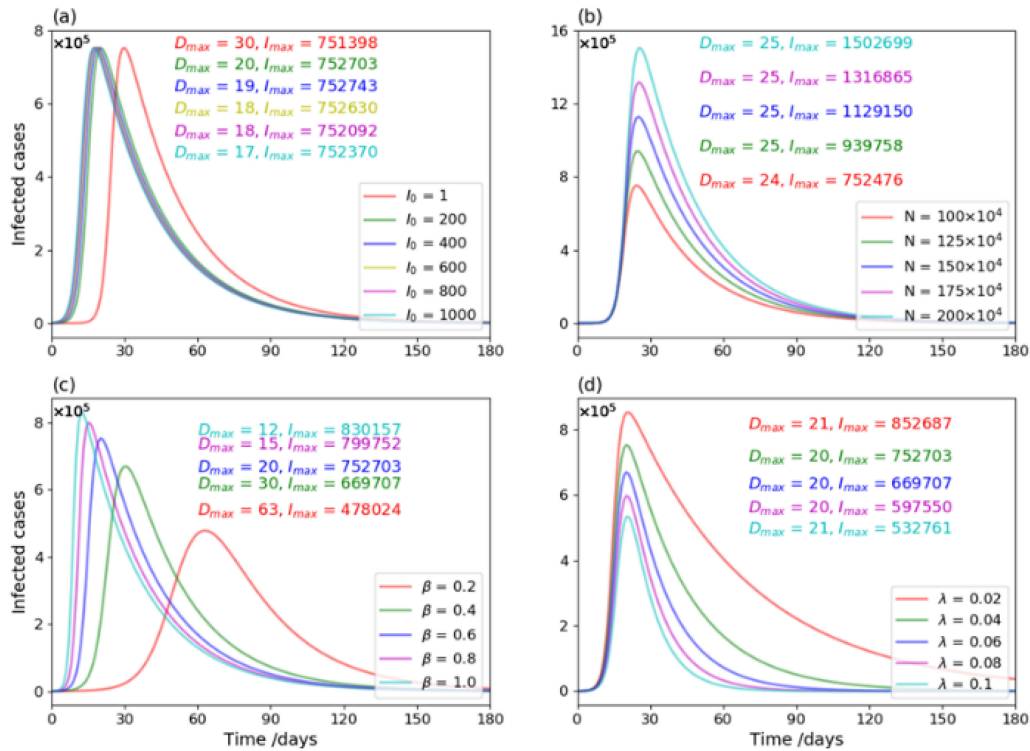


Fig. 1. Variation in the infected population (simulated by SIR) with the variation in the initial actively infected cases (I_0 , Fig. 1a), the total number of the population (N , Fig. 1b), infectious rate (β , Fig. 1c), and cure rate (λ , Fig. 1d). The initial state variables, parameters, and outputs of the model vary by the same interorders of magnitude.

Given that the total population is 1 million and β and λ are fixed as 0.6 and 0.04, respectively, it is observed that I_{max} almost does not change when I_0 varies from 1 to 1000, but D_{max} is reached 10 days earlier when I_0 varies from 1 to 200 and 2–3 days earlier when I_0 varies from 200 to 1000 (Fig. 1a), suggesting that I_0 has limited influence on I_{max} but that a larger I_0 leads to a quick peak of the pandemic; thus, the response time is very limited, which requires extremely quick action to prevent and control the spread of the pandemic.

When N (which can be regarded as the community size) varies from 1 million to 2 million, I_{max} proportionally increases from approximately 0.75 million to 1.5 million, but D_{max} changes only minimally (Fig. 1b), suggesting that the community size is critically sensitive to actively infected cases; that is, a larger community causes many more infected cases. Thus, closing the community and keeping infected cases in a smaller community can effectively prevent the spread of the pandemic.

Although the analysis of the initially infected cases and the community size based on a specific SIR model, their influences on the spread of the pandemic are general. The initially infected cases represent the base number of the infected cases, which are the “seed” or “source” of the transmission chain. More initially infected cases mean more transmission sources. In a specific community, more initially infected cases may make the more people of the community (even the whole community) get infected, i.e., the D_{max} arrives more quickly. Community size represents the number of people who will be potentially infected. The larger of the community size, the more people

may be infected, and they may become newly initially infected cases. Thus, isolating the infected cases in a smaller community can effectively block the spread of the pandemic in the larger community.

With β increasing from 0.2 to 1.0, I_{max} almost doubles, and D_{max} occurs substantially earlier (moving from the 63rd day to the 12th day) (Fig. 1c), suggesting that the infection rate is very sensitive to both I_{max} and D_{max} . Reducing the infection rate can reduce the number of infected cases and postpone the pandemic peak date but can make the pandemic last longer, i.e., flatten the curve of the pandemic.

With λ increasing from 0.02 to 0.1, D_{max} has almost no change, but I_{max} decreases obviously and quickly (from 852687 cases to 532761 cases, Fig. 1d), suggesting that parameter λ influences I_{max} and decreases the speed of the actively infected cases. This means that increasing the cure rate could effectively reduce the maximum number of actively infected cases and potentially stop the pandemic.

Experiment 2: Here, we change the values of the initial state variables and parameters at interorders of magnitude to see the variations in the model outputs (Fig. 2). Under fixed β ($= 0.6$) and λ ($= 0.04$), approximately 75% of the total population is infected regardless of the initial infected cases and the total number of susceptible populations. Both a smaller number of initial infected cases and larger communities would result in a much more long-lasting pandemic.

When the initial number of actively infected cases is magnified twenty-thousand-fold (Fig. 2a), there is almost no difference

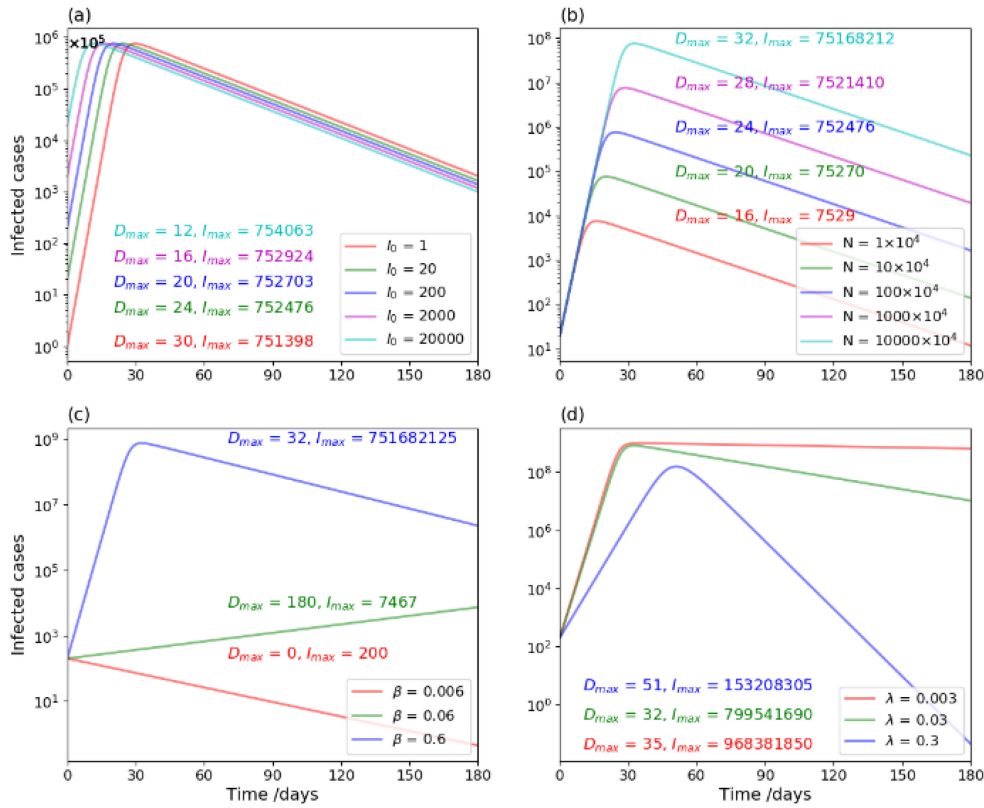


Fig. 2. Variation in the infected population (simulated by SIR) with the variation in the initial infected cases (I_0 , Fig. 2a), the total number of the population (N, Fig. 2b), infectious rate (β , Fig. 2c), and cure rate (λ , Fig. 2d). The initial state variables, parameters, and outputs of the model vary over orders of magnitude.

in I_{max} , which approximately equals 75% of the total population, but it shortens the pandemic period by approximately half a month, indicating that the more initially infected cases there are, the earlier the pandemic peak is reached and the earlier the pandemic is completed.

As the community size (N) increases (e.g., from 10000 at a village/street level to 100 million at a country level), the number of actively infected cases expands proportionally, and the pandemic lasts much longer (Fig. 2b), indicating that if the actively infected cases are isolated in a very small community, the pandemic could exhaust itself quickly, with a very small number of people infected. Thus, isolating the community and controlling the total susceptible population is one of the most effective measures to stop and control the pandemic outbreak.

As seen from Fig. 2c, if β is reduced to 10% of the original value (taking 0.6 as an original value), the pandemic cannot reach the peak value of the actively infected cases in half a year, and if β is reduced to 1% of the original value, the pandemic does not occur. This means that large changes in β over interorders of magnitude lead to the pandemic developing in completely different ways.

Similarly, if λ is reduced to 10% of the original value (taking 0.3 as an original value, Fig. 2d), D_{max} moves ahead significantly with I_{max} growing over fivefold, and if λ is reduced to 1% of the original value, D_{max} also moves ahead, and I_{max} grows continuously. Both conditions lead to a much longer pandemic.

Experiment 3: For the SEIR model, the sensitivities of four parameters, α , β , γ , and δ , on the infected (dashed line in Fig. 3) and cumulative cases (solid line in Fig. 3) are analyzed. Due to the intervention measures applied, both infected and cumulative cases are dramatically reduced.

As seen from Fig. 3a, even in the case of low α , I_{max} is approximately 1965, accounting for less than 0.2% of the total population (1 million), and the cumulative cases number less than 8000, accounting for 0.8% of the total population. With α increasing, both infected and cumulative cases decrease significantly, suggesting that the application of protection measures can significantly reduce the actively and totally infected cases.

With β doubling (e.g., 0.5 to 1.0), the numbers of both actively infected and cumulative cases triple, and D_{max} moves earlier (from the 19th day to the 14th day) (Fig. 3b), indicating that the infection rate is still sensitive to the actively infected cases and peak date in the SEIR model, which is consistent with what has been observed in the SIR model except that much smaller populations are infected with the protection measures being applied in the SEIR model.

When γ increases, both infected and cumulative cases increase dramatically (Fig. 3c), suggesting that a larger γ leads to a smaller D_{max} and larger I_{max} ; that is, a shortened incubation time causes a very quick spread of the pandemic, with the peak date being quickly reached.

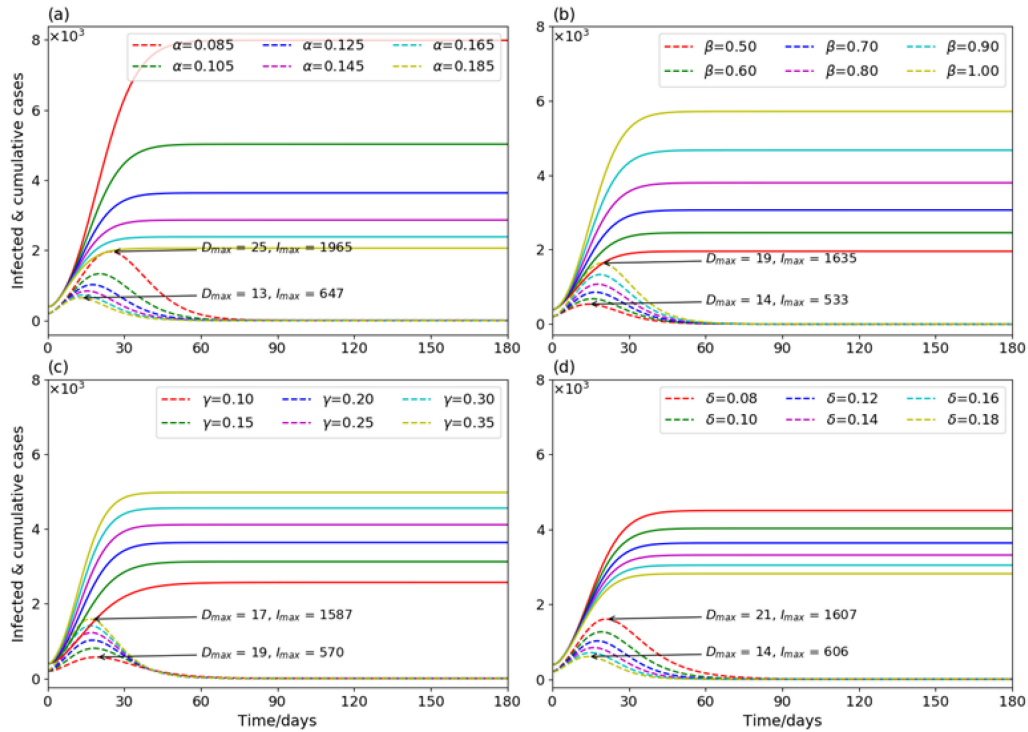


Fig. 3. Variation in the actively infected (dashed line) and cumulative (solid line) populations (simulated by SEIR) with variation in α , β , γ , and δ .

The effect of δ on the actively affected and cumulative cases is opposite to that of γ , i.e., with increasing δ , both the actively infected and cumulative cases decrease, and D_{max} is reached earlier (Fig. 3d). This suggests that the longer the time from onset to isolation, the longer the pandemic duration and the more people infected.

B. Parameter Sensitivity Based on Global Method

Parameter sensitivities on infected and cumulative cases simulated by the SEIR model, as well as on the basic reproduction number (R_0), are shown in Fig. 4 and Table III. First, both Sobol's and FAST methods show highly consistent parameter sensitivity indices on the three targets (I , C and R_0), which indicates that the sensitivity analysis based on two different methods derives reliable and reasonable results.

For the infected and cumulative populations, α shows the most sensitive effects, with its first-order sensitivities on the infected and cumulative populations being 0.415 and 0.559, respectively, meaning that the protection rate dominates the infected and cumulative cases. This observation is highly consistent with that observed in experiment 3; thus, combining local and global sensitivity analysis, we suggest that improving the protection rate is of utmost importance to control and prevent further outbreaks of the pandemic.

The parameter δ^{-1} is also sensitive to the number of infected populations, ranking 2nd place, with the first-order sensitivity index being 0.17, suggesting that quarantined time (duration from one infection to one quarantine) is a key factor influencing the spread of the pandemic and that applying quarantine measures as early as possible is the most effective way to control

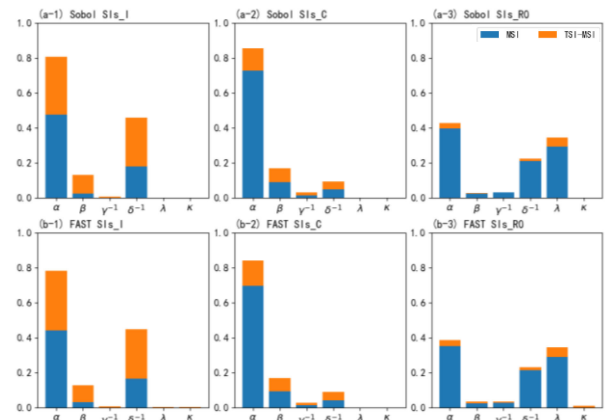


Fig. 4. Parameter SIs from Sobol's and FAST methods on infected and cumulative populations and basic reproduction number (R_0). The main sensitivity index, total sensitivity index, and interactive effects are represented by the MSI (blue bar), TSI (blue plus orange bar), and TSI-MSI (orange bar), respectively.

the pandemic because increasing δ^{-1} causes more infected cases and longer pandemic duration.

The parameter γ^{-1} is sensitive to the total number of cumulative cases, ranking 2nd with a first-order sensitivity index of 0.101, suggesting that incubation time is an important indicator that represents the transmission speed of the pandemic. A shortened incubation time makes the disease spread more quickly, and allows more people to be infected; thus, a fast response and the application of isolation and protection are critically important.

The parameter β was ranked 3rd in both actively infected (Fig. 4a-1 and 4b-1) and cumulative cases (Fig. 4a-2 and 4b-2),

TABLE III

PARAMETER SIs TO THE INFECTED AND CUMULATIVE CASES, AS WELL AS THEIR RANKS ACCORDING TO THE FIRST-ORDER INDICES

Model output	Parameters	MSI	TSI	Interaction	Rank
Actively infected cases	α	0.415	0.805	0.389	1
	β	0.019	0.121	0.103	3
	γ^{-1}	0.006	0.067	0.061	4
	δ^{-1}	0.170	0.504	0.334	2
Cumulative cases	α	0.559	0.785	0.226	1
	β	0.067	0.163	0.096	3
	γ^{-1}	0.101	0.245	0.144	2
	δ^{-1}	0.032	0.079	0.046	4
RO	α	0.398	0.403	0.005	1
	β	0.004	0.004	0.000	4
	γ^{-1}	0.004	0.004	0.000	5
	δ^{-1}	0.217	0.219	0.002	3
	λ	0.379	0.388	0.009	2

which is consistent with observations from local sensitivity analysis, suggesting that the infectious rate is influential and should be carefully addressed through applying isolation and improving protection to reduce the infectious rate and hence to prevent the spread of the pandemic.

For the basic reproduction number (RO), α , λ and δ^{-1} are the first three most sensitive parameters, with the summation of their first-order sensitivities greater than 0.9 (Fig. 4a-3 and 4b-3). This means that the protection rate, cure rate and average quarantined time are the dominant factors that govern the behavior the the basic reproduction number. Also, infectious rate β and average incubation γ^{-1} have a certain influence on RO , which should be carefully addressed. Different from other state variables (e.g., I, C) in SEIR models, the RO is synthetically influenced by multiple parameters, thus, comprehensively assessing its influence on the pandemic is critical important. From this point, the global sensitivity analysis presented in study well supports the existing consensus on the importance of RO [29]–[31].

Overall, the SIs and importance rank of the parameter suggest that improving the protection rate α is the most effective method and enhancing quarantine and incubation measures are especially important to control the transmission of the pandemic because shortened incubation time leads to faster signing of the symptoms and more cumulative cases in a short time, while a long quarantine time produces a longer pandemic with more people infected. Besides, the cure rate is also influential to the basic reproduction number, i.e., a higher cure rate may lead to a smaller basic reproduction number, hence, to end the pandemic earlier.

In addition to the first order and total effects of the parameter, the interactions among parameters also influence the number of actively infected and cumulative cases. Both α and δ^{-1} show significant interactions, as seen in Fig. 4 and Table III. By calculating the second-order sensitivity index, we further identify that the interactions of α and δ^{-1} mainly come from mutual

TABLE IV

SUMMARY OF THE SENSITIVITY ANALYSIS AND IMPLICATIONS FOR PREVENTION AND CONTROL OF THE PANDEMIC

	Sensitivity	Interaction with other parameters	Implication for prevention and control of the pandemic
N	Very sensitive to the number of actively infected cases and the date of the maximum number of cases	--	Reducing the total population exposed to the virus (e.g., via isolation, tracing the actively infected cases) can reduce both the infected population and the pandemic during.
I_0	Weakly sensitive to the date of the maximum number of cases	--	More initially actively infected cases in a specific size of community may reach the peak and end the pandemic earlier, i.e., reaching herd immunity.
α	Very sensitive to both the number of infected and the number of cumulative cases	Very strong with δ^{-1} , poor with β and γ^{-1}	Synthetically increasing the protection rate and quarantine time ends the pandemic earlier with fewer people infected.
β	1. Very sensitive to the number of actively infected cases without intervention applied (i.e., SIR) 2. Weakly sensitive to the number of actively infected cases with intervention applied (i.e., SEIR).	1. Not applicable 2. Poor with α	Reducing the infectious rate at the very beginning might decrease the number of actively infected cases. Applying synthetic measures of control infectious rate and improving protection rate can be an effective way to control the pandemic.
γ^{-1}	Sensitive to cumulative cases	Poor with α	Prolonging the incubation time ends the pandemic later but with a smaller cumulative number of people infected, i.e., flattening the curve.
δ^{-1}	Sensitive to actively infected cases	Very strong with α	Synthetically increasing protection rate and quarantine time ends the pandemic earlier with fewer people infected.

interaction. Parameters α and δ^{-1} share the largest interaction, with values greater than 0.33. This means that the protection rate and average quarantine time do not affect the number of actively infected cases in a separate manner but in a coeffect manner. This observation requires that we cannot separately rely on strategy but coordinately increase the protection rate and average quarantine time to prevent and control pandemics.

C. Dynamical Variation in Parameter Sensitivity

Fig. 5 shows parameter SIs on the actively infected cases that present significant variation at different stages. For the infected population, the main sensitivity index of parameter α first increases, reaching the maximum value at the early stage of the pandemic (e.g., 25th–30th day), and then decreases (Fig. 5a), while the total effect of the parameter maintains high values

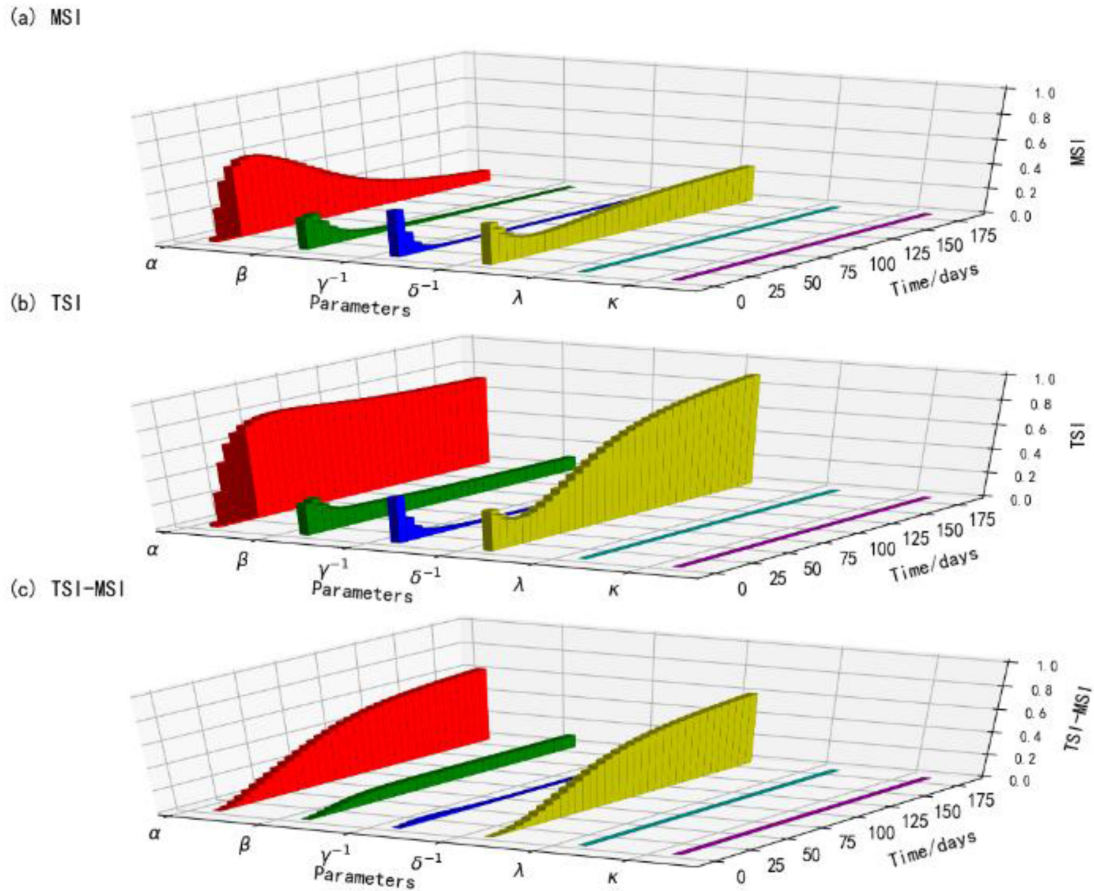


Fig. 5. Dynamic variation in the parameter SIs measured by Sobol's method under the full ranges of the parameters. With the evolution of time, the parameters' main SIs (a), total SIs (b), and differences between the total and main SIs (c) change dramatically.

after reaching a maximum value at the 25th–30th day (Fig. 5b). These observations mean that the role that the protection rate plays is most significant in the first month of the pandemic transmission period, and this role is played solely by the parameter (i.e., the main sensitivity index) gradually decreasing, while the role jointly played by α and other parameters (i.e., interaction effects shown in Fig. 5c) are always high. This suggests that the parameter α is particularly significant to model output on the 25th–30th day, that protection measures should be taken as early as possible, and that after the 30th day, the improvement of the protection rate should be combined with other measures (e.g., isolation).

With the spread of the pandemic, the effects of infectious rate β on infected and cumulative populations decrease sharply and are significant in the first half month to one month. This means that it is of utmost importance to control the infection rate for the first half month to one month, after which efforts may be less effective. Parameter γ^{-1} is sensitive to the number of infected populations at the very beginning of the pandemic. This suggests that the average incubation time at the early stage is especially important for controlling the transmission speed of the pandemic. Combined with the effects of parameter δ^{-1} on the infected population, these results suggest that implementing

quarantine measures as early as possible is a promising way to control the transmission of the pandemic.

The interaction among parameters quantified by the global sensitivity analysis is an important indicator that quantifies the coefficient of multiple parameters on the model output (e.g., infected and cumulative cases). This is also an important factor for making decisions on the synthetic use of multiple measures to prevent and control the pandemic. For example, although the main effect of α on actively infected cases is not as strong at the latter stage of the pandemic, its interactive effect and total effects are clearly significant. Additionally, the interactive effects of α and δ^{-1} increase substantially with the development of the pandemic. We have demonstrated that the interaction arises solely from α and δ^{-1} . Thus, synthetic measures (increasing protection rate and average quarantine time) should be applied to quantify multiple factors rather than a single factor to control the pandemic.

IV. CONCLUSION

The sensitivities of the parameters, initial values of the state variables, and community size of the SIR-type model are analyzed, and their implications for the prevention and control of

the pandemic are provided in Table IV. The most significant findings are summarized as follows.

By analyzing the sensitivity of N , we show that a larger community size leads to not only many more actively infected cases but also a much longer pandemic duration, indicating that closing the community and isolating actively infected cases in a small community where very limited people are exposed to the virus is the most effective way to stop the spread of the pandemic. This finding suggests that if actively infected cases are isolated in a very small community, the pandemic could quickly pass with a very small number of people infected.

We find that the infection rate is the most influential parameter dominating the behavior of the SIR-type model (i.e., without applying intervention). The infection rate strongly influences both the number of actively infected cases and the date on which the maximum number of actively infected cases is reached, and the cure rate influences the maximum number of actively infected cases. Reducing the infectious rate and increasing the cure rate could effectively control the outbreak of the pandemic but make the pandemic last longer, i.e., flattening the curve of the pandemic. In addition, we find that the initial value of actively infected cases influences the number of actively infected cases, i.e., a larger initial value of actively infected cases also makes the pandemic last longer.

Parameters α and δ^{-1} in the modified SEIR model are most sensitive to the infected population, with a summation of their first-order SIs being 0.585 and their interactions being greater than 0.33. The high first-order sensitivities and interaction between α and δ^{-1} indicate that we should not only focus on the effect of a single parameter but also synthetically apply an increasing protection rate and average quarantine time to prevent and control the pandemic.

REFERENCES

- [1] G. Giordano et al., "Modelling the COVID-19 epidemic and implementation of population-wide interventions in Italy," *Nature Med.*, vol. 26, pp. 855–860, 2020.
- [2] Y. Fang, Y. Nie, and M. Penny, "Transmission dynamics of the COVID-19 outbreak and effectiveness of government interventions: A data-driven analysis," *J. Med. Virol.*, vol. 92, no. 6, pp. 645–659, Jun. 2020.
- [3] J. T. Wu et al., "Estimating clinical severity of COVID-19 from the transmission dynamics in Wuhan, China," *Nature Med.*, vol. 26, no. 4, pp. 506–510, Apr. 2020.
- [4] S. J. Barnes, "Information management research and practice in the post-COVID-19 world," *Int. J. Inf. Manage.*, vol. 55, Jul. 2020, Art. no. 102175.
- [5] W. He, G. Y. Yi, and Y. Zhu, "Estimation of the basic reproduction number, average incubation time, asymptomatic infection rate, and case fatality rate for COVID-19: Meta-analysis and sensitivity analysis," *J. Med. Virol.*, vol. 92, no. 11, pp. 2543–2550, 2020.
- [6] R. K. Rai et al., "Impact of social media advertisements on the transmission dynamics of COVID-19 pandemic in India," *J. Appl. Math. Comput.*, vol. 68, no. 1, pp. 19–44, Feb. 2022.
- [7] F. Liu, X. Li, and G. Zhu, "Using the contact network model and metropolis-hastings sampling to reconstruct the COVID-19 spread on the 'Diamond Princess,'" *Sci. Bull.*, vol. 65, no. 15, pp. 1297–1305, 2020.
- [8] Z. Yang et al., "Modified SEIR and AI prediction of the epidemics trend of COVID-19 in China under public health interventions," *J. Thoracic Dis.*, vol. 12, no. 3, pp. 165–174, 2020.
- [9] Z. Zhao et al., "Prediction of the COVID-19 spread in African countries and implications for prevention and control: A case study in South Africa, Egypt, Algeria, Nigeria, Senegal and Kenya," *Sci. Total Environ.*, vol. 729, Aug. 2020, Art. no. 138959.
- [10] A. J. Kucharski et al., "Early dynamics of transmission and control of COVID-19: A mathematical modelling study," *Lancet Infect. Dis.*, vol. 20, no. 5, pp. 553–558, 2020.
- [11] S. Khajanchi and K. Sarkar, "Forecasting the daily and cumulative number of cases for the COVID-19 pandemic in India," *Chaos: Interdiscipl. J. Nonlinear Sci.*, vol. 30, no. 7, 2020, Art. no. 071101.
- [12] S. Khajanchi et al., "Mathematical modeling of the COVID-19 pandemic with intervention strategies," *Results Phys.*, vol. 25, Jun. 2021, Art. no. 104285.
- [13] G. Giordano et al., "Modelling the COVID-19 epidemic and implementation of population-wide interventions in Italy," *Nature Med.*, vol. 26, no. 6, pp. 855–860, Jun. 2020.
- [14] K. Sarkar, S. Khajanchi, and J. J. Nieto, "Modeling and forecasting the COVID-19 pandemic in India," *Chaos, Solitons Fractals*, vol. 139, Oct. 2020, Art. no. 110049.
- [15] Y. C. Chen, P.-E. Lu, C.-S. Chang, and T.-H. Liu, "A time-dependent SIR model for COVID-19 with undetectable infected persons," *IEEE Trans. Netw. Sci. Eng.*, vol. 7, no. 4, pp. 3279–3294, Oct.–Dec. 2020.
- [16] Z. Tang, X. Li, and H. Li, "Prediction of new coronavirus infection based on a modified SEIR model," 2020, to be published, doi: [10.1101/2020.03.03.20030858](https://doi.org/10.1101/2020.03.03.20030858).
- [17] S. H. A. Khoshnaw, R. H. Salih, and S. Sulaimany, "Mathematical modelling for coronavirus disease (COVID-19) in predicting future behaviours and sensitivity analysis," *Math. Modelling Natural Phenomena*, vol. 15, 2020, Art. no. 33.
- [18] G. R. Phaijoo and D. B. Gurung, "Sensitivity analysis of SEIR–SEI model of dengue disease," *GAMS J. Math. Math. Biosci.*, vol. 6, pp. 41–50, 2018.
- [19] M. Naveed et al., *Dynamical Behavior and Sensitivity Analysis of a Delayed Coronavirus Epidemic Model*. Berlin, Germany: Springer, 2020.
- [20] R. Resmawan and L. Yahya, "Sensitivity analysis of mathematical model of coronavirus disease (COVID-19) transmission," *Cauchy*, vol. 6, no. 2, pp. 91–99, 2020.
- [21] S. Marino et al., "A methodology for performing global uncertainty and sensitivity analysis in systems biology," *J. Theor. Biol.*, vol. 254, no. 1, pp. 178–196, Sep. 2008.
- [22] S. M. Kassa, J. B. H. Njagarah, and Y. A. Terefe, "Modelling Covid-19 mitigation and control strategies in the presence of migration and vaccination: The case of South Africa," *Afrika Matematika*, vol. 32, no. 7, pp. 1295–1322, Nov. 2021.
- [23] S. M. Kassa, J. B. H. Njagarah, and Y. A. Terefe, "Analysis of the mitigation strategies for COVID-19: From mathematical modelling perspective," *Chaos Solitons Fractals*, vol. 138, Sep. 2020, Art. no. 109968.
- [24] I. Ghosh, "Within host dynamics of SARS-CoV-2 in humans: Modeling immune responses and antiviral treatments," *SN Comput. Sci.*, vol. 2, no. 6, Oct. 2021, Art. no. 482.
- [25] E. Borgonovo and X. Lu, "Is time to intervention in the COVID-19 outbreak really important? A global sensitivity analysis approach," 2020, to be published, doi: [10.48550/arXiv.2005.01833](https://doi.org/10.48550/arXiv.2005.01833).
- [26] G. Chowell et al., "Model parameters and outbreak control for SARS," *Emerg. Infect. Dis.*, vol. 10, no. 7, 2004, Art. no. 1258.
- [27] T. Zhou et al., "Preliminary prediction of the basic reproduction number of the Wuhan novel coronavirus 2019-nCoV," *J. Evidence-Based Med.*, vol. 13, no. 1, pp. 3–7, 2020.
- [28] P. Samui, J. Mondal, and S. Khajanchi, "A mathematical model for COVID-19 transmission dynamics with a case study of India," *Chaos Solitons Fractals*, vol. 140, Nov. 2020, Art. no. 110173.
- [29] S. Khajanchi, S. Bera, and T. K. Roy, "Mathematical analysis of the global dynamics of a HTLV-I infection model, considering the role of cytotoxic T-lymphocytes," *Math. Comput. Simul.*, vol. 180, pp. 354–378, 2021.
- [30] Y. Alimohamadi, M. Taghdir, and M. Sepandi, "Estimate of the basic reproduction number for COVID-19: A systematic review and Meta-analysis," *J. Prev. Med. Public Health*, vol. 53, no. 3, pp. 151–157, 2020.
- [31] J. Ma, "Estimating epidemic exponential growth rate and basic reproduction number," *Infect. Dis. Modelling*, vol. 5, pp. 129–141, Jan. 2020.
- [32] X. Li, F. Liu, and M. Fang, "Harmonizing models and observations: Data assimilation in Earth system science," *Sci. China Earth Sci.*, vol. 63, no. 8, pp. 1059–1068, 2020.
- [33] X. Li, Z. Zhao, and F. Liu, "Big data assimilation to improve the predictability of COVID-19," *Geography Sustainability*, vol. 1, no. 4, pp. 317–320, Dec. 2020.
- [34] W. O. Kermack and A. G. McKendrick, "A contribution to the mathematical theory of epidemics," in *Proc. Roy. Soc. London. Ser. A, Containing Papers Math. Phys. Character*, 1927, pp. 700–721.

- [35] L. Peng *et al.*, "Epidemic analysis of COVID-19 in China by dynamical modeling," 2020, to be published, doi: [10.48550/arXiv.2002.06563](https://doi.org/10.48550/arXiv.2002.06563).
- [36] I. M. Sobol, "Global sensitivity indices for nonlinear mathematical models and their Monte Carlo estimates," *Math. Comput. Simul.*, vol. 55, no. 1-3, pp. 271–280, Feb. 2001.
- [37] I. M. Sobol', "Sensitivity estimates for nonlinear mathematical models," *Math. Modelling Comput. Experiments*, vol. 4, pp. 407–414, 1993.
- [38] A. Saltelli, S. Tarantola, and K. P.-S. Chan, "A quantitative model-independent method for global sensitivity analysis of model output," *Technometrics* vol. 41, no. 1, pp. 39–56, 1999.
- [39] C. Ma, X. Li, and S. Wang, "A global sensitivity analysis of soil parameters associated with backscattering using the advanced integral equation model," *IEEE Trans. Geosci. Remote Sens.*, vol. 53, no. 10, pp. 5613–5623, Oct. 2015.
- [40] C. Ma, X. Li, J. Wang, C. Wang, Q. Duan, and W. Wang, "A comprehensive evaluation of microwave emissivity and brightness temperature sensitivities to soil parameters using qualitative and quantitative sensitivity analyses," *IEEE Trans. Geosci. Remote Sens.*, vol. 55, no. 2, pp. 1025–1038, Feb. 2017.
- [41] R. Cukier *et al.*, "Study of the sensitivity of coupled reaction systems to uncertainties in rate coefficients. Part I theory," *J. Chem. Phys.*, vol. 59, no. 8, pp. 3873–3878, 1973.
- [42] U. Nguemdjo *et al.*, "Simulating the progression of the COVID-19 disease in Cameroon using SIR models," *PLoS One*, vol. 15, no. 8, 2020, Art. no. e0237832.